EPiC Series in Computing

Volume 104, 2024, Pages 193–208

Proceedings of 3rd International Workshop on Mathematical Modeling and Scientific Computing

3D Cellular Automata-Based Model of Bacterial Biofilm Formation with Developed Surface Spreading Mechanism

Anna G. Maslovskaya[1,2]*, Samvel K. Sarukhanian[3]†, and Christina Kuttler[4]‡

[1] Innopolis University, Innopolis, Russia
a.maslovskaya@innopolis.ru
[2] Kazan Federal University, Kazan, Russia
[3] Amur State University, Blagoveshchensk, Russia
saruhanyans@gmail.com
[4] Technical University of Munich, Garching, Germany
kuttler@ma.tum.de

Abstract

Cellular automata, being an apparatus for the implementation of discrete dynamic models, play a special role in mathematical biology and *in silico* studies of microorganisms. The study was undertaken to design 3D hybrid cellular automata-based model of bacterial biofilm taking into account the surface spreading mechanism. The model formalization is based on the cellular automaton algorithm of biofilm evolution, a discrete analogy for the diffusion model of nutrient consumption, and an additional inoculation mechanism. The proposed computational procedure allows to conduct simulations under variations of key model parameters: the initial nutrient level, the probability of additional inoculation, and the radius of random inoculation transfer. A series of *in silico* experiments was conducted to investigate biofilm formation with a focus on ensuring two key factors: maximum space occupation with minimal resource consumption.

1 Introduction

The *in silico* study of major groups of microorganisms has recently gained high importance due to modern challenges from viruses and pathogen bacteria. Biofilms are the predominant life-form of bacteria (estimates suggest that 99% of all bacteria exist in biofilm communities), which provides for this survival. The formation of biofilms is a sophisticated and meticulously controlled process where bacteria attach to surfaces and create organized, multicellular communities. These biofilms can emerge on a wide range of surfaces, including medical devices, natural habitats, and human tissues. Bacterial biofilms possess a complex structure. Approximately 20% of the biofilm's volume is encased within an extracellular matrix that fills up to 80% of the structure. This matrix contains channels for the transport of nutrients and oxygen, as well as

*Provided methodology, developing model, writing – original draft
†Designed algorithm and implemented software, validation, visualization
‡Did supervision, conceptualization, writing – review & editing

V.L. Turova, A.E. Kovtanyuk and J. Zimmer (eds.), MMSC 2024 (EPiC Series in Computing, vol. 104), pp. 193–208

for the removal of waste products [5]. For certain bacteria, such as those belonging to the genus *Pseudomonas*, the development of stable macrostructures is initiated or influenced by "quorum sensing" as a relevant mechanism of bacterial communication [20, 33]. The formation of biofilms provides for the enhancement of virulence factors in many bacteria, as well as the development of resistance to antibacterial medicine. The significance of studying biofilm evolution arises from the need to control the population of pathogenic bacteria, predict the level of resistance to antimicrobial agents and disinfectants, and establish standards for the maintenance of medical equipment to reduce the risk of nosocomial infections. Hence, comprehending the mechanisms of biofilm formation is essential for identifying effective strategies for treating infections caused by pathogens.

When investigating bacterial behavior and aiming to control infections, two fundamental challenges emerge. Modeling bacterial growth: We must create accurate representations of how bacteria multiply and consume nutrients in their surroundings. This involves developing mathematical models that simulate bacterial biomass increase in different nutrient media. [15, 19, 25]. Unraveling quorum sensing: bacterial communities often communicate and coordinate their actions through a process called "quorum sensing". We need to fully understand the mechanisms of this communication system, as it significantly influences how bacteria behave, including their ability to form biofilms, produce toxins, and develop resistance to antibiotics [8, 22, 23, 28, 32, 35], and the development of biofilm structures. The latter, in turn, can be based on a variety of model concepts provided by deterministic, stochastic, and agent-based approaches [17]. Deterministic time-dependent continuous models of microorganism growth are mostly formalized with the use of partial differential equations and allow simulating evolution of biofilm structure, in particular under the influence of external conditions, such as temperature, pH, oxygen, and nutrient factors, or antimicrobial agents [3, 7, 12, 13]. The stochastic approach to modeling bacterial biofilm evolution is based on Monte-Carlo simulation of microbial populations and randomness in behavior such as the probability of mutations (as an example, the Gillespie algorithm and the Markov chain Monte-Carlo method are noted in [14]). In general, agent-oriented models presume the use of individual-based simulation or cellular automaton algorithms. Individual-based models permit one to simulate the individual behavior and wide range of interactions between microorganisms [1, 21].

As an alternative methodology for biofilm modeling, the theory of cellular automata can be applied. Cellular automata have become a powerful tool for modern simulations, serving as a fundamental building block for a wide array of discrete-dynamical models across various fields. This popularity can be attributed to advancements in information technology, the availability of high-performance computing, the rise of interactive 3D modeling systems, and the clarity and visual interpretability they offer in solving real-world problems. Cellular automata models have proven particularly useful in understanding biological systems, including disease spread, tissue and cell growth in organisms, and microbial community interactions [10, 18].

In the context of microbial systems, each cell in a cellular automaton model represents an individual organism or element within a biofilm. The interaction rules within these models determine how cells behave and interact with each other and their environment. This enables researchers to analyze various aspects of biofilm growth, such as morphology, thickness, growth rate, response to environmental changes, and dynamics of nutrient and oxygen consumption. Cellular automata for biofilms find applications in biomedical and biotechnological research, facilitating the development of strategies to control and manage biofilm evolution [4, 11]. Various research groups have developed cellular automaton-based models for these purposes [13, 21, 27, 30, 31]. A hybrid approach to modeling biofilm structure, combining a continuous model for nutrient transport with a discrete cellular automaton model for individual

cell behavior, has been proposed [27]. This approach offers a powerful way to capture both the macroscopic and microscopic aspects of biofilm dynamics.

An original algorithm assumes a numerical solution of a differential problem to estimate the evolution of nutrition for a discretized region, each element of which represents a fragment of the biofilm structure. This model includes control parameters of the biosystem that determine the adequacy of the model to observed processes. The study [13] highlights how fluid flow patterns (hydrodynamics) significantly influence the distribution of nutrients and the resulting spatial structure of biofilms. The model proposed in [21] demonstrates the importance of individual cell behavior in the formation of biofilm structure and dynamics, emphasizing the need for individual-based approaches in understanding biofilm formation. In [29], a classical cellular automaton has been introduced to simulate the formation of a bacterial film from the point of view of formalizing the rules of "life" of a discrete structure. Numerous processes that accompany the formation of bacterial structures (nucleation, division, erosion, death) have been formalized to create realistic scenarios for the evolution of the biosystem. As a consequence, the complex formalization of the algorithm involves consideration of lattices of small dimensions. However, the process of creating a unified concept of cellular automata modeling of the evolution of biological films is far from complete. This is due to the fact that the simulated systems belong to classes that are difficult to formalize and are distinguished by the heterogeneity of their biocomposition, the diversity of genetic material, and the composition of self-organization factors, the consequence of which is the formation of this dense structure.

In our previous studies, we designed and implemented 2D and 3D cellular automaton models of bacterial biofilm formation [31]. The proposed algorithms have been based on simple rules for modeling the spatial self-similar evolution in bacterial biofilm populations and specifying geometric characteristics of porosity for visualized fractal aggregates. However, bacterial inoculation during the formation of a biofilm plays a potent role in the process of occupying the available area containing the resource that supports the vital activity of these microorganisms. In this regard, the relevant problem with the functionality of the model includes the special procedure for bacterial surface spread during the evolution of biofilm.

This research focuses on enhancing a 3D cellular automaton model for simulating bacterial biofilm formation. The model incorporates a surface spreading mechanism, capturing how bacteria expand across surfaces. The key innovation is a hybrid algorithm that introduces rules for simulating biofilm evolution realistically. These rules prioritize two crucial factors. Maximum space occupation: the model incorporates an additional inoculation mechanism that ensures bacteria effectively occupy available space. Minimal resource consumption: the model minimizes the amount of resources required by the bacteria, reflecting their need for efficient survival. By integrating these factors, the model provides a more accurate and realistic representation of biofilm development, contributing to a deeper understanding of bacterial behavior and the potential for controlling biofilm formation in various applications.

2 The conceptualization of microbiological system

Many bacteria, when living freely in their environment, have the ability to attach to surfaces, whether these are living (biotic) or non-living (abiotic). If the conditions are right, this attachment can lead to the formation of organized, complex, three-dimensional communities of bacteria, known as biofilms. Biofilms are held together by special substances called organic microbial polymers. These polymers act like glue, helping the bacterial cells stick together and to their surroundings. The formation of a biofilm occurs in a series of stages [34]. The most important ones are shown in Fig. 1.

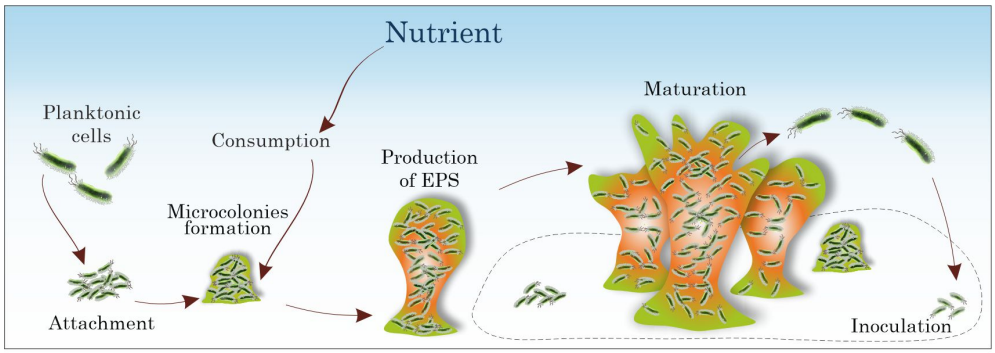

Figure 1: The typical development stages of a biofilm community.

The first stage of biofilm formation involves individual bacteria, known as planktonic cells, moving around and attaching to a surface. This initial attachment is weak and reversible, meaning the bacteria can easily detach again. These initial attachments are often facilitated by forces like Van der Waals forces and hydrophobic effects [9].

After the initial contact, bacteria produce an extracellular polymeric matrix (EPS), which anchors them more securely to the surface, making the attachment irreversible. Immersion of bacteria in secreted EPS provides the necessary conditions for biofilm maturation and progress. As the biofilm matures, the bacteria multiply and produce more EPS, creating a complex, three-dimensional structure. This stage is marked by the formation of water channels that allow nutrients and waste to be transported within the biofilm [6, 16, 26]. Finally, the fully mature biofilm reaches its maximum cell density and can release microcolonies and single cells to colonize new environments or new locations.

In the present study, the main focus was on the dispersal mechanism of biofilm formation. The dispersal mechanism in bacterial biofilms is critically important because it facilitates the spread of bacteria from the established biofilm to new environments, thereby contributing to the colonization of new surfaces, the initiation of new infections, the increase of resistance to treatments, genetic diversity, and environmental adaptation and the persistence of bacterial populations in dynamic environments [2, 24].

Based on previous studies [27, 31], we will develop here a hybrid model of bacterial biofilm evolution, which includes the following two foremost approaches: discrete-dynamical simulation of a biofilm evolution and discrete analogies of time-dependent deterministic-continuous models for the nutrient distributions and the consumption of nutrients by biomass.

Let us assume that a computational domain is represented by a confined space, namely a rectangular parallelepiped with defined dimensions. This space is filled with a nutrient solution containing a specific, hypothetical nutrient. Initially, individual bacterial cells are randomly dispersed onto the bottom surface of the simulated environment. As time progresses, these bacteria interact with each other and begin to grow, forming a larger mass. This growth process consumes nutrients from the environment. The total nutrient concentration can be unlimited as well as limited and controlled. The concentration of nutrients is numerically estimated during the system dynamics. Also, we suppose the absence of inhibitory factors.

In this study, we used a combination of approaches to model bacterial behavior and growth. 3D Cellular automata: we represent individual bacterial cells and their interactions using 3D cellular automata, a powerful tool for simulating complex systems at the cellular level.

Discrete analogies of the Monod equation: we employ discrete versions of the Monod equa-

tion, a well-established model for bacterial growth, to define how the growth rate of bacteria depends on the availability of nutrients. Diffusion equation: we use the diffusion equation to simulate how nutrients spread and become available to the bacteria in the simulated environment. This combined approach allows us to capture the dynamics of bacterial growth and nutrient consumption realistically.

The process is observed for a fixed time, after which we measure the density of the bottom surface coverage, the quantity and concentration of biomass, the remaining nutrient level, and the fractal dimension of the resulting structure.

3 Model description

Let's delve into the specifics of our designed cellular automaton-based hybrid model for simulating biofilm-forming bacterial populations. This section will outline the core principles of how the cellular automaton operates, including defining the fundamental elements and structure of the model and setting up the initial arrangement of cells in the 3D space by establishing the rules that determine how cells change state and interact within the model.

3.1 Grid geometry

Basically, models based on cellular automaton algorithms are discrete-dynamical models, which permit us to formalize various biological systems. Following the cellular automaton approach, each discrete element can be defined using states and all states are discrete and finite. A cell of a cellular automaton grid can change state due to rules of local interaction. In this matter, truncated octahedra can be applied to define the shape of the basic cells of the constructed 3D cellular automaton. The truncated octahedron is a polyhedron with 14 faces (6 squares and 8 hexagons), which offers a unique and powerful approach for modeling 3D phenomena using cellular automata (CA). The truncated octahedron exhibits isotropic behavior, meaning it has equal properties in all directions. This is crucial for ensuring that the CA model does not favor any particular direction, leading to more realistic and unbiased simulations. Truncated octahedra perfectly fill 3D space, eliminating gaps and ensuring smooth transitions between cells, unlike simpler shapes like cubes. This contributes to a more accurate representation of spatial dynamics in simulations. The truncated octahedron has 14 neighbors, which can be categorized into different layers (direct neighbors, second-layer neighbors, etc.). This complexity enables one to implement sophisticated interaction rules between cells, capturing realistic interactions within a 3D environment. The structure of the truncated octahedron permits it to be readily adjusted by altering the relative sizes of its square and hexagonal faces, offering flexibility in adapting the model to specific physical constraints or complexities.

However, the use of the truncated octahedron brings some challenges, such as the increased number of neighbors can lead to increased computational complexity, especially for large-scale simulations and implementation complexity. In addition, we should stress that the truncated octahedron offers a compelling alternative to traditional cubical cells in 3D cellular automata. Its isotropic, space-filling nature and complex neighbor relationships provide a powerful tool for accurately capturing realistic 3D phenomena in various fields like biofilm modeling, fluid dynamics, and materials science. While implementing a 3D cellular automaton model presents certain challenges, the benefits it offers in terms of realism and detail outweigh these complexities. This makes it a promising approach for developing sophisticated and insightful simulations of 3D phenomena.

Neighboring of node schematically illustrated in Fig. 2. We define the rules for transitioning from an element with an index $[i, j, k]$ to Cartesian space.

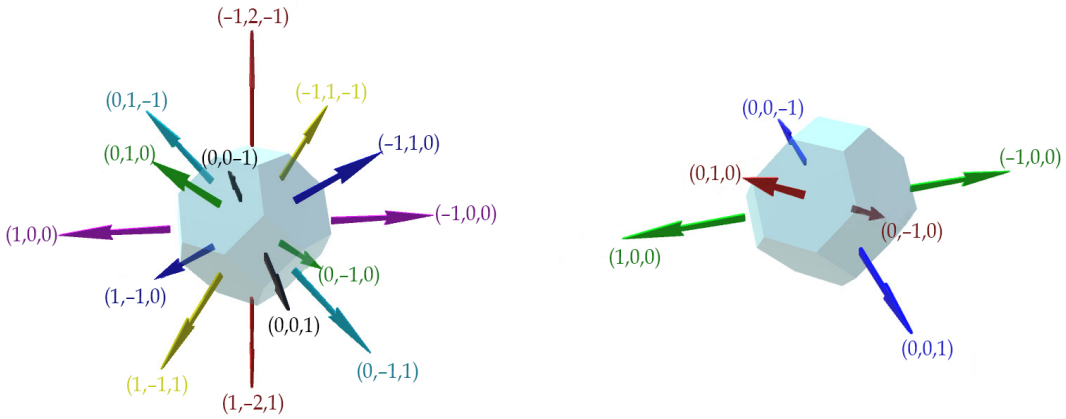

(a) (b)

Figure 2: Planes directions associated with the neighbors and corresponding basis vectors for a truncated octahedron cell.

Figure 2 shows all neighbor directions for a truncated octahedron node (a) and basis vector directions for the node (b). Neighboring vectors are used for division and interaction, while basis vectors are used to calculate position.

The following expression can be used for calculating the position of a node defined by vector v according to its indices i, j, and k and basis vectors a_i:

$$v(i,j,k) = i\vec{a_1} + j\vec{a_2} + k\vec{a_3}, \quad where \quad \begin{cases} \vec{a_1} = (2,0,0), \\ \vec{a_2} = (1,1,1), \\ \vec{a_3} = (0,0,2). \end{cases} \tag{1}$$

3.2 Identifying cellular automata rules

To formalize the rules of operation of the cellular automaton, let us introduce here several preliminary remarks and do some assumptions. In the context of biology, the term “cell” has two meanings. To avoid confusion, we will use the term “unit” to refer to the nodes in the cellular automaton grid. The term “cell” will be applied concerning bacterial cells (specifically, “cell” refers to a populated “unit”). For the sake of simplicity in our model setup and analysis, we have chosen to not explicitly model the extracellular polymeric substance (EPS) matrix, which is a key component of biofilms. Instead, we assume that bacterial cells are already embedded within this matrix. We also don’t consider the secretion of EPS beyond this initial assumption. To further simplify, we will treat a single unit within our cellular automaton model as representing a specific amount of biomass, essentially a group of bacterial cells rather than a single cell. This allows us to focus on the overall dynamics of bacterial growth and interaction without getting bogged down in the complexities of individual cell behavior.

Therefore, we will consider the dynamic finite cellular automaton, which is formalized by the triple of objects:

$$< X, A, \Theta >, \tag{2}$$

where X is the set of automaton units; A is a finite set of unit states; Θ is a set of operators of transition for various unit states related to the unit configuration.

We define the set of units X as follows:

$$X = \{[0,0,0],[1,0,0],...,[l,0,0],[0,1,0],...,[l,w,h]\}. \tag{3}$$

In this way, the set of units is indexed along the basis axes: l denotes the length of the computational domain, w is the width, and h is the height. The finite set of unit states can be specified as:

$$A = \begin{cases} C_b - \text{the bacterial mass concenctration}, \\ C_s - \text{the nutrient mass concentration}. \end{cases} \tag{4}$$

Each unit of the grid is characterized by a bacterial biomass concentration C_b and a nutrient concentration C_s. At the initialization phase, the value of C_b is set to the initial value $C_{b,init}$ of a unit. From the beginning, the initial values of the bacterial concentration, C_b equals zero for each unit of the grid, apart from defined units at the bottom of the computation domain, for which we inoculated bacterial cells with the initial value C_{b0}.

We assume that diffusion occurs uniformly in all directions. This assumption is made because the units share faces, unlike the diagonal neighbors of a cube. While it would be more realistic to model how the presence of bacterial biomass within cells affects nutrient diffusion, this would significantly increase the complexity of our calculations. Therefore, for the sake of simplicity, we've chosen to omit this aspect from our model.

The set of transition operators between different unit states can be defined as follows:

$$\Theta([i,j,k]) = (\theta_{dif}[i,j,k], \theta_{cons}[i,j,k], \theta_{div}, \theta_{spread}, \theta_{push}), \tag{5}$$

where $\theta_{dif}[i,j,k]$ is the transition operator related to mass-balance operators to define nutrient concentration; $\theta_{cons}[i,j,k]$ is the transition operator for nutrient consumption by a bacterial cell; θ_{div} is the transition operator to specify border cell division; θ_{spread} is the transition operator attributed to the occupation of available space due to inoculation; θ_{push} is the transition operator related to division mechanism due to inner cells.

To ensure that the amount of nutrients remains consistent throughout our simulation, we utilize Fick's law. This law helps us describe how the concentration of nutrients changes over time and space. Specifically, we use a general diffusion equation to model the movement of each nutrient component:

$$\frac{\partial C_s}{\partial t} = D\Big(\frac{\partial^2 C_s}{\partial x^2} + \frac{\partial^2 C_s}{\partial y^2} + \frac{\partial^2 C_s}{\partial z^2}\Big), \tag{6}$$

where the general notation C_s is related to the nutrient concentration value; D is the diffusion coefficient.

Further, we apply equation (6) to estimate the concentrations of nutrient components by the following rules for the cellular automaton:

$$\theta_{dif}[i,j,k]: \quad C_s[i,j,k,t+\delta t] = C_s[i,j,k,t] + D\Big(\sum_{m=1}^{M} C_s(m,t) - MC_s[i,j,k,t]\Big), \tag{7}$$

where $C_s(m,t)$ is a nutrient concentration of m-th neighbor of the unit at the iteration which corresponds to the time t; M is the total number of neighbors around the unit.

The recalculation of biomass and nutrient concentrations is given using the following rules:

$$\theta_{cons}[i,j,k] : \begin{cases} J[i,j,k] = \mu_{max} \frac{C_s[i,j,k]}{\left(K_s + C_s[i,j,k]\right)}, \\ C_s[i,j,k] = C_s[i,j,k] - J[i,j,k], \\ C_b[i,j,k] = C_b[i,j,k] + J[i,j,k], \end{cases} \tag{8}$$

where J is the uptake rate of nutrient concentration by bacteria; μ_{max} (known as the Michaelis constant) is the maximum specific growth rate of the microorganism and K_s is the "half-velocity constant", which represents saturation constant of considered nutrient type.

In addition, the rule used to define the biomass division is followed by:

$$\theta_{div}[i,j,k] : \begin{cases} C_b[i,j,k] = C_b[i,j,k]/2, \\ C_b[i_{new}, j_{new}, k_{new}] = C_b[i,j,k]/2, \end{cases} \tag{9}$$

where $i_{new}, j_{new}, k_{new}$ are coordinates for the new populated cell, which is neighboring to the considered cell i,j,k (the position of a new cell is selected randomly from the available set of positions).

This rule is implemented only for cells, which meet the following conditions:

$$\begin{cases} C_b[i_{new}, j_{new}, k_{new}] = 0, \\ C_b[i,j,k] > C_{div}. \end{cases} \tag{10}$$

This implementation is possible for cells with a sufficiently high biomass concentration $C_b[i,j,k]$ and if it has a free neighbor $C_b[i_{new}, j_{new}, k_{new}]$. The transition operator θ_{push} is related to the pushing mechanism implemented when all neighboring units are occupied, and there is no possibility of dividing into neighboring units. In this case, for simplicity, we assume that a unit (to realize the division process) is chosen randomly from the set of all unoccupied neighbors of cells located on the biofilm boundary.

The transition operator θ_{spread} corresponds to the spreading mechanism, which proceeds as follows. First, we check the condition that the randomly selected number is less than the probability parameter of the spread, and there is at least one unpopulated unit amongst the units at the bottom of the region in the vicinity of an inoculating cell. This implies that a random unit is selected amongst available units at the bottom of the area to realize the inoculation process. By assumption, the vicinity of the region is a linearly dependent parameter on the height of the inoculating cell.

In our model setup, we have assumed that the boundaries of our computational domain are far enough away from the active areas where bacteria are growing that they don't significantly influence the processes happening within the model. Therefore, we've simplified our calculations by not taking boundary effects into account. Furthermore, we update all the grid units in our model simultaneously during each step of the simulation. This approach means that all changes within the grid are applied at the same time, rather than sequentially.

4 Computational experiment results and discussion

The following section collects the procedure and the outcome of the algorithms.

4.1 Algorithmization and software implementation aspects

By this statement, let us formalize the designed algorithm and determine the main processes controlling the dynamics of the biosystem. Figure 3 illustrates the flowchart of the algorithm.

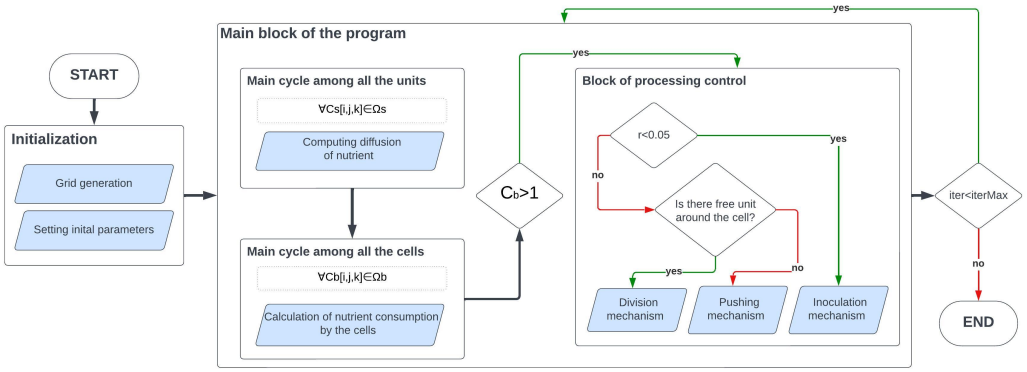

Figure 3: The flowchart of the algorithm.

In the initial step, we initialize all parameters and generate the cellular automaton lattice. Further, the main computation cycle is performed which includes two subcycles. The first subcycle calculates the nutrient distribution for all units in the lattice according to (7). The second subcycle is intended for all populated units (cells). In this case, the amount of nutrient consumption is calculated for each cell. After that, the nutrient concentration in the cell decreases while the bacterial mass concentration rises (8). Furthermore, if the biomass concentration of a cell has reached the value necessary for division, one of the possible mechanisms of division is selected. Primarily, we specify the possibility of inoculation by drawing a random number and placing it within the confidence interval with an *a priori* established probability. If inoculation is impossible due to probability, then, depending on the presence of free space, the division mechanism is carried out (there is the possibility of division with relocation to an adjacent unit) or the pushing mechanism is applied otherwise. After the implementation of the main cycle, we increment the iteration index related to the time in simulations and check if it has reached the maximum value (144000 in the computational experiments).

In the present study, we apply Unity and C# to perform simulation due to Unity's 3D rendering engine, which allows to visualize complex scientific data. The 3D model of biofilm growth involves a large amount of data and its processing. Here is a breakdown of the key aspects of the implementation. Independent computational modules: cellular automata algorithms are well-suited for parallelization because each unit operates independently, relying only on its immediate neighbors.The C# language provides built-in features like "Parallel" for implementing parallel algorithms. This allows for efficient execution by utilizing multiple processor cores. The model uses "Parallel.For" and "Parallel.Foreach" loops to execute tasks in parallel, speeding up the simulation process. To prevent conflicts when multiple threads access the same data simultaneously, the model incorporates lock objects, ensuring data integrity. This parallelization approach significantly improves performance, specifically for simulating diffusion processes, resulting in a 30-40% reduction in execution time. Biomass concentration threshold: each cell in the model tracks its biomass concentration. When a cell reaches a sufficient level, it searches

for a neighboring cell to divide into. If multiple available neighbors exist, the cell randomly chooses one for division. The dividing cell increases the biomass concentration in the designated neighbor cell, effectively creating a new cell. Newly created cells are added to a separate list. After iterating through all cells, the new cells are rendered visually and incorporated into the master list, while the temporary new cell list is cleared. This approach effectively prevents continuous recalculation of new cells, avoiding unnecessary looping and improving efficiency. The simulation system effectively predicts the spatial and temporal distribution of bacterial populations within biofilms. The model can analyze and evaluate the geometrical characteristics of surface roughness, providing insights into biofilm formation. The software implementation is enhanced with a user interface, making it more user-friendly and accessible.

4.2 Simulation of biofilm growth

As part of computational experiments, we will set the goal of identifying patterns of biofilm growth depending on the spreading process and conditions of nutrition limitation. Thus, when conducting computational experiments, it is necessary to vary the control parameters of the model, such as the level of initial nutrition, the probability of inoculation, and the initial localization of the colony that affect the spatial-temporal distributions of bacterial biomass. To assess the level of complexity and porosity of the structure, we will use the calculation of the fractal dimension of the biofilm boundaries. In the computational experiments, we use dimensional parameters to estimate spatial nutrient distribution and nutrient consumption by bacteria. At the same time, we apply relative units to discrete-dynamical simulations of the processes of biomass spreading due to inoculation, division, and pushing mechanisms. The "real" time unit is associated with the iteration number $Iter$ and the space unit is related to the specific cellular automaton non-dimensional normalized unit (named as "CA unit"). Table 1 lists the set of key simulation parameters. We stress that most parameters rely on the conditions of experiments and the surrounding environment, such as bacterial strain, temperature, liquid viscosity, pH level, oxygen, etc.

Parameter	**Symbol**	**Value**	**Units**
CA length	L	100	CA units
CA width	W	100	CA units
CA height	H	100	CA units
Initial nutrient concentration	$C_{s,init}$	2-7 $\times 10^{-3}$	kg $\cdot$ m^{-3}
Initial number of cells	n_0	1-100	CA units
Maximum biomass growth rate	μ_{max}	4.2 $\times 10^{-9}$	h^{-1}
Diffusion coefficient	D	2.1 $\times 10^{-9}$	m$^2\cdot$ s^{-1}
Half-saturation constant	K_s	3.1 $\times 10^{-3}$	kg $\cdot$ m^{-3}
Spreading probability	p_{spread}	0-5	%

Table 1: Simulation parameters.

To initialize the three-dimensional computational domain, we generated an area bounded by a parallelepiped with linear dimensions L, W, H. Within the framework of the cellular automata model, a corresponding lattice was generated based on the cell of a truncated octahedron. We assumed that at the initial moment of time, bacterial seeding was carried out at the bottom of the area in places with a certain location.

The implementation of a hybrid cell-automaton-based model with support for software implementation allows one to visualize the dynamics of spatial evolution of biomass, and two-dimensional sections, as well as evaluate the characteristics of biomass and the fractal dimension of structure boundaries.

Figures 4 – 5 illustrate the 3D simulation results of bacterial biofilm formation under a variation of key parameters: initial nutrient concentration, spreading probability, number, and location of initial cells. Specifically, Fig. 4(a) demonstrates the effect of the spreading mechanism. Here we set only one bacterial colony at the central position of the computational domain and assume the situation when we have rather rich nutrient conditions. We can observe that the colony actively reproduces when nutrients are available, forming a fairly dense dendrite structure. Turning on the spreading mechanism (possibility of inoculation) leads to the occupation of the entire accessible area. We can indicate a more uniform structure that completely covered the bottom of the area.

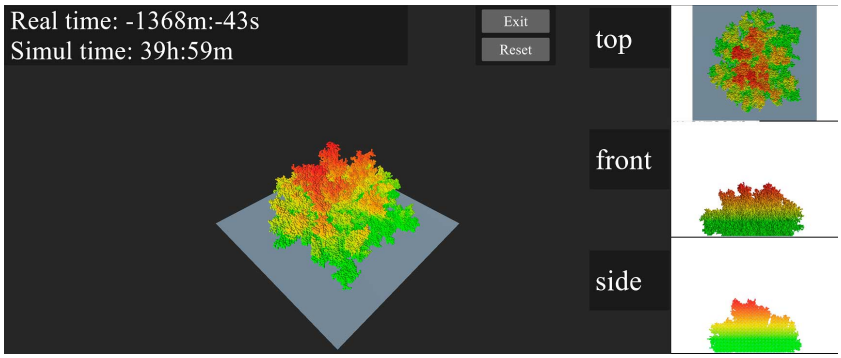

(a)

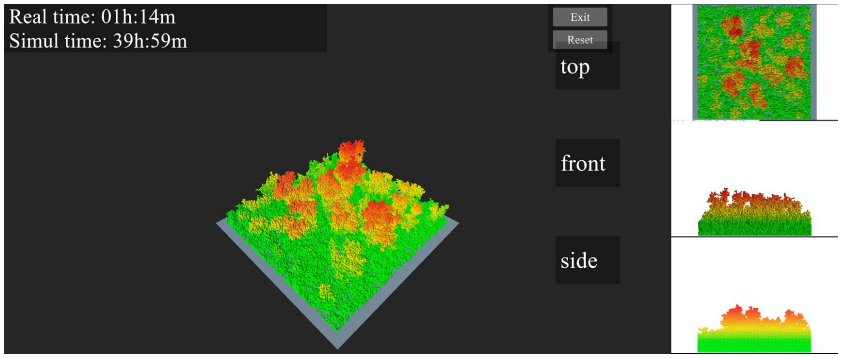

(b)

Figure 4: Spatial biofilm structures: the simulation results at $C_{s,init} = 70$ and one colony initially for $p_{spread} = 0$ – (a), $p_{spread} = 5\%$ – (b). Color distributions correspond to different heights: from the lowest (green) to the highest (red).

Figure 5 is related to the analysis of spreading mechanism effects under the condition of low initial nutrients. In this case, we initially placed 100 colonies randomly distributed in a geometric region representing a circle with a radius equal to a quarter of the linear size of the region. Simulation results suggest that saving nutrition is a limiting factor for biofilm growth even in the presence of an inoculation process. The formed structures also have a dendrite-like structure, but the colonies are more scattered and the porosity of the biomass is quite high.

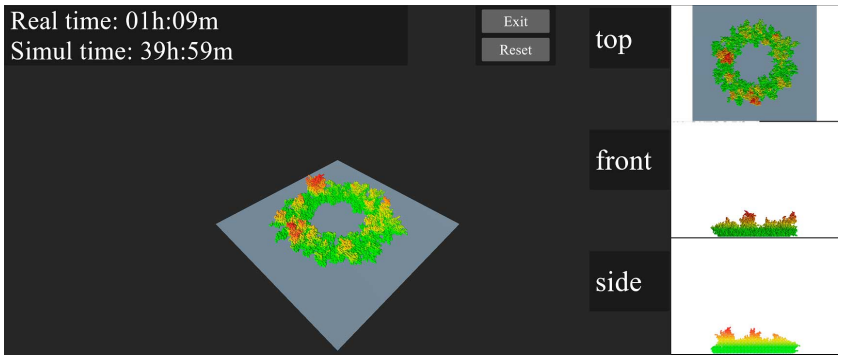

(a)

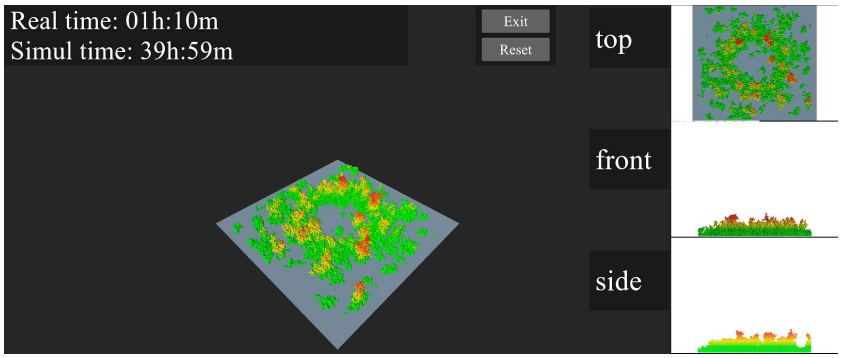

(b)

Figure 5: Spatial representation of biofilm: simulation results at $C_{s,init} = 30$ and 100 colonies at start moment for $p_{spread} = 0$ – (a), $p_{spread} = 1\%$ – (b). Color distributions correspond to different heights: from the lowest (green) to the highest (red).

In the aspect of studying the numerical characteristics of the biofilm structure, we will take as a basis two integral values, namely the surface density and the fractal dimension of the biofilm boundaries. The numerical estimation of surface density (as shown in Fig. 6) is performed as the sum of all cells located at the bottom plane divided by the sum of all units located at the bottom. To calculate the fractal dimension of biofilm structures, we apply the classical "box-counting" method. Here we will perform computations for the case of one initially generated colony placed at the central position of the computational domain. The presented data indicate the relationship between the key factors that determine the film's occupation of possible space. It is important to note that only a sufficient level of inoculation and increased nutrition give the combined effect of the formation of dense structures.

Figure 7 shows the dependence of the fractal dimension of the three-dimensional biofilm structure on the probability of spreading for different values of the initial nutrient concentration. The initial nutrient level plays a significant role in the complexity of the biofilm geometry. As it increases, the structure forms more complex patterns in terms of fractal dimension. With an increasing probability of spreading, the value of the fractal dimension decreases, which can be explained by more uniform coverage of the area.

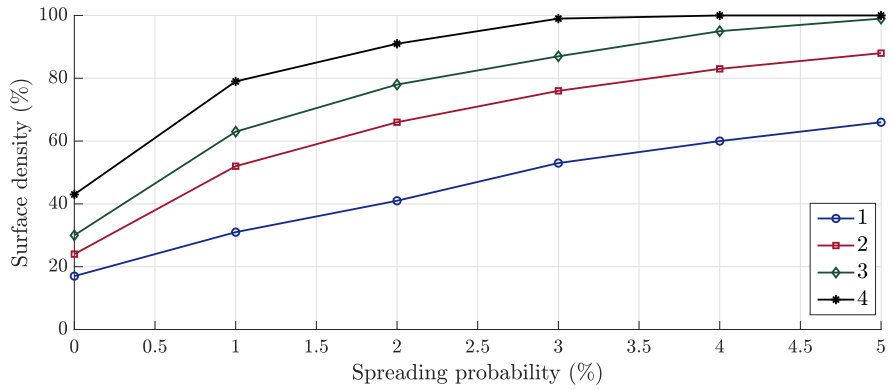

Figure 6: Surface density as a function of spreading probability for different initial nutrient levels: $C_{s,init} = 100\%$ – (1), $C_{s,init} = 70\%$ – (2), $C_{s,init} = 50\%$ – (3), $C_{s,init} = 30\%$ – (4).

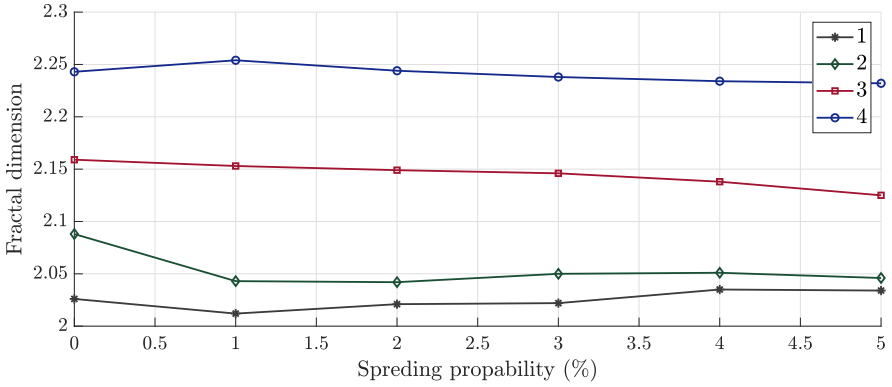

Figure 7: Fractal dimension as a function of spreading probability for different values of initial nutrient concentrations: $C_{s,init} = 30\%$ – (1), $C_{s,init} = 50\%$ – (2), $C_{s,init} = 70\%$ – (3), $C_{s,init} = 100\%$ – (4).

Figure 8 depicts changes in the surface density over time-related to iterations in the program application. We can observe that the surface is completely covered by 35000 iterations in case of the high initial nutrient concentration (100%) and the value of spreading probability $p = 5\%$ while "turning off" the inoculation mechanism at maximum nutrient level results in only a 30% level of bacterial surface density. Furthermore, our findings suggest that over time, the inoculation mechanism, even with a low nutrient level, can lead to more overgrowth of the surface than with a high nutrient level without a spreading mechanism.

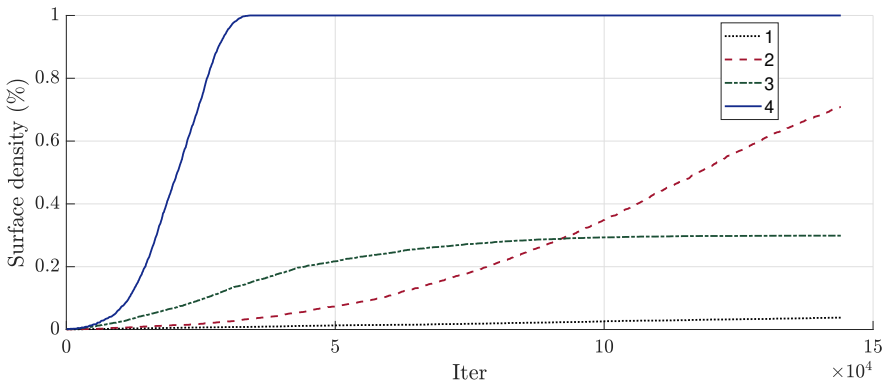

Figure 8: The dynamics of surface density as a function of program iterations for different values of the initial nutrient concentration and spreading probability: $C_{s,init} = 30\%$, $p_{spread} = 0\%$ – (1), $C_{s,init} = 30\%$, $p_{spread} = 5\%$ – (2), $C_{s,init} = 100\%$, $p_{spread} = 0\%$ – (3), $C_{s,init} = 100\%$, $p_{spread} = 5\%$ – (4).

5 Conclusion

Taken together, the current study summarizes the result of design of the hybrid 3D cellular automata-based model for biofilm evolution in the view of the surface spreading mechanism. Using the Unity software environment, we implemented the algorithm for modeling biofilm growth under the conditions of limited nutrient supply with the ability to control the inoculation process. Our findings confirm that the relevant parameters are presented by the initial nutrient concentration and the probability of spreading. The initial nutrient level is the primary factor affecting the size and structure of the biofilm. Nevertheless, a long-term effect is observed in the priority of the contribution of control parameters to the processes of surface overgrowth changes. The results of this study can be relevant for the optimization of the growth and spread of bacterial colonies in a variety of applications, such as bioremediation and the production of biofuels. The prospect of future research is the formalization of bacterial quorum sensing, which is a trigger for the processes of inoculation and the formation of dense resistant biofilms.

6 Acknowledgments

The study has been supported by the Ministry of Science and Higher Education of Russia (project no. 122082400001-8) and the Kazan Federal University (the Strategic Academic Leadership Program “PRIORITY-2030”).

References

[1] E. Alpkvist, C. Picioreanu, M. C. M. van Loosdrecht, and A. Heyden. Three-dimensional biofilm model with individual cells and continuum EPS matrix. *Biotechnology and Bioengineering*, 94:961–979, 2006.

[2] B. R. Boles and A. R. Horswill. *Staphylococcal* biofilm disassembly. *Trends in Microbiology*, 19:449–455, 2011.

[3] J. D. Chambless, S. M. Hunt, and P. Stewart. A three-dimensional computer model of four hypothetical mechanisms protecting biofilms from antimicrobials. *Applied and Environmental Microbiology*, 72(2):1406–1416, 2006.

[4] X. Chen and P. Stewart. Modeling the architecture of dehydrated microbial biofilms. *Applied Biochemistry and Biotechnology*, 119:69–94, 2004.

[5] J. W. Costerton, Z. Lewandowski, D. Caldwell, D. Korber, and H. Lappin-Scott. Microbial biofilms. *Annual Review of Microbiology*, 50:711–745, 1996.

[6] D. Davies. Understanding biofilm resistance to antibacterial agents. *Nature Reviews Drug Discovery*, 2:114–122, 2003.

[7] M. A. Delavar and J. Wang. *Advanced Methods and Mathematical Modeling of Biofilms: Applications in Health Care, Medicine, Food, Aquaculture, Environment, and Industry.* Academic Press, 2022.

[8] J. D. Dockery and J. P. Keener. A mathematical model for quorum sensing in *Pseudomonas aeruginosa*. *Bulletin of Mathematical Biology*, 63(1):91–116, 2001.

[9] R. Donlan and J. Costerton. Biofilms: survival mechanisms of clinically relevant microorganisms. *Clinical Microbiology Reviews*, 15:167–193, 2002.

[10] R. M. Donlan. Biofilms: Microbial life on surfaces. *Emerging Infectious Diseases*, 8:881–890, 2002.

[11] K. Drescher, J. Dunkel, and C. D. Nadell. Architectural transitions in *Vibrio cholerae* biofilms at single-cell resolution. *Proceedings of the National Academy of Sciences of the USA*, 113:E2066–E2072, 2016.

[12] R. Duddu, S. Bordas, D. Chopp, and B. Moran. A combined extended finite element and level set method for biofilm growth. *International Journal for Numerical Methods in Engineering*, 74:848–870, 2008.

[13] H. J. Eberl, C. Picioreanu, J. J. Heijnen, and M. C. M. van Loosdrecht. A three-dimensional numerical study on the correlation of spatial structure, hydrodynamic conditions, and mass transfer and conversion in biofilms. *Chemical Engineering Science*, 55:6209–6222, 2000.

[14] D. T. Gillespie. Exact stochastic simulation of coupled chemical reactions. *The Journal of Physical Chemistry*, 81(25):2340–2361, 1977.

[15] I. Golding, Y. Kozlovsky, I. Cohen, and E. Ben-Jacob. Studies of bacterial branching growth using reaction-diffusion models for colonial development. *Physica A: Statistical Mechanics and its Applications*, 260:510–554, 1998.

[16] L. Hall-Stoodley, J. Costerton, and P. Stoodley. Bacterial biofilms: from the natural environment to infectious diseases. *Nature Reviews Microbiology*, 2:95–108, 2004.

[17] H. Horn and S. Lackner. Modeling of biofilm systems: a review. *Advances in Biochemical Engineering/Biotechnology*, 146:53–76, 2014.

[18] H. Kasamatsu and D. Barry. *Biofilm and Materials Science.* Springer, 2015.

[19] K. Kawasaki, A. Mochizuki, M. Matsushita, N. Shigesada, and T. Umeda. Modeling spatio-temporal patterns generated by *Bacillus subtilis*. *Journal of Theoretical Biology*, 188(2):177–185, 1997.

[20] T. D. Kievit. Quorum sensing in *Pseudomonas aeruginosa* biofilms. *Environmental Microbiology*, 11(2):279–306, 2009.

[21] J. Kreft, C. Picioreanu, J. Wimpenny, and M. C. M. van Loosdrecht. Individual-based modelling of biofilms. *Microbiology*, 147:2897–2912, 2001.

[22] C. Kuttler and A. Maslovskaya. Hybrid stochastic fractional-based approach to modeling bacterial quorum sensing. *Applied Mathematical Modelling*, 93:360–375, 2021.

[23] C. Kuttler and A. Maslovskaya. Computer-assisted modelling of quorum sensing in bacterial population exposed to antibiotics. *Frontiers in Applied Mathematics and Statistics*, 8:951783, 2022.

[24] D. McDougald, S. A. Rice, N. Barraud, P. D. Steinberg, and S. Kjelleberg. Should we stay or

should we go: mechanisms and ecological consequences for biofilm dispersal. *Nature Reviews Microbiology*, 10:39–50, 2011.

[25] M. Mimuraa, H. Sakaguchib, and M. Matsushita. Reaction-diffusion modelling of bacterial colony patterns. *Physica A: Statistical Mechanics and its Applications*, 282:283–303, 2000.

[26] G. O'Toole, H. Kaplan, and R. Kolter. Biofilm formation as microbial development. *Annual Review of Microbiology*, 54:49–79, 2000.

[27] C. Picioreanu, M. C. M. van Loosdrecht, and J. J. Heijnen. Mathematical modeling of biofilm structure with a hybrid differential-discrete cellular automaton approach. *Biotechnology and Bioengineering*, 58:101–116, 1998.

[28] J. Pérez-Velázquez and R. Gómez-Gómez. Mathematical modelling of bacterial quorum sensing: a review. *Bulletin of Mathematical Biology*, 78:1585–1639, 2016.

[29] D. Rodriguez, A. Carpio, and B. Einarsson. A cellular automata model for biofilm growth. In *10th World Congress on Computational Mechanics*, volume 1, pages 409–421. Blucher Mechanical Engineering Proceedings, 2014.

[30] D. Rodriguez, B. Einarsson, and A. Carpio. Biofilm growth on rugose surfaces. *Physical Review E*, 86(6):061914, 2012.

[31] S. Sarukhanian, A. Maslovskaya, and C. Kuttler. Three-dimensional cellular automaton for modeling of self-similar evolution in biofilm-forming bacterial populations. *Mathematics*, 11:3346, 2023.

[32] Y. Shuai, A. Maslovskaya, and C. Kuttler. 2D reaction-diffusion model of quorum sensing characteristics during all phases of bacterial growth. *Far Eastern Mathematical Journal*, 22(2):232–237, 2022.

[33] F. F. Tuon, L. R. Dantas, P. H. Suss, and V. S. T. Ribeiro. Pathogenesis of the *Pseudomonas aeruginosa* biofilm: A review. *Pathogens*, 11(3):300, 2022.

[34] A. D. Verderosa, M. Totsika, and K. E. Fairfull-Smith. Bacterial biofilm eradication agents: A current review. *Frontiers in Chemistry*, 9:5451, 2021.

[35] J. Ward and N. Balaban. Mathematical modeling of quorum-sensing control in biofilms. In *Control of Biofilm Infections by Signal Manipulation*, pages 79–108. Springer, 2008.